AIP | Applied Physics Letters

Mechanism of the enhancement of mid-infrared emission from GeS2-Ga2S3 chalcogenide glass-ceramics doped with Tm3+

Changgui Lin, Shixun Dai, Chao Liu, Bao'an Song, Yinsheng Xu, Feifei Chen, and Jong Heo

Citation: Applied Physics Letters **100**, 231910 (2012); doi: 10.1063/1.4727900
View online: http://dx.doi.org/10.1063/1.4727900
View Table of Contents: http://scitation.aip.org/content/aip/journal/apl/100/23?ver=pdfcov
Published by the AIP Publishing

Articles you may be interested in

Upconversion luminescence in Er3+ doped Ga10Ge25S65 glass and glass-ceramic excited in the near-infrared
J. Appl. Phys. **113**, 083520 (2013); 10.1063/1.4793638

Near-infrared down-conversion in rare-earth-doped chloro-sulfide glass GeS2–Ga2S3–CsCl: Er, Yb
J. Appl. Phys. **110**, 113107 (2011); 10.1063/1.3665638

New far-infrared transmitting Te-based chalcogenide glasses
J. Appl. Phys. **110**, 043536 (2011); 10.1063/1.3626831

Intense near-infrared and midinfrared luminescence from the Dy 3 + -doped GeSe 2 – Ga 2 Se 3 – MI (M = K , Cs, Ag) chalcohalide glasses at 1.32, 1.73, and 2.67 μ m
J. Appl. Phys. **109**, 033105 (2011); 10.1063/1.3531555

Modified local environment and enhanced near-infrared luminescence of Sm 3 + in chalcohalide glasses
Appl. Phys. Lett. **89**, 131117 (2006); 10.1063/1.2357939

Want to publish your paper in the
#1 MOST CITED journal in applied physics?
With *Applied Physics Letters*, you can.

AIP | Applied Physics Letters

THERE'S POWER IN NUMBERS. Reach the world with AIP Publishing.

This article is copyrighted as indicated in the article. Reuse of AIP content is subject to the terms at: http://scitation.aip.org/termsconditions. Downloaded to IP: 141.223.173.110 On: Wed, 22 Apr 2015 08:35:40

Mechanism of the enhancement of mid-infrared emission from GeS_2-Ga_2S_3 chalcogenide glass-ceramics doped with Tm^{3+}

Changgui Lin,[1,2] Shixun Dai,[2,a)] Chao Liu,[3] Bao'an Song,[2] Yinsheng Xu,[1,2] Feifei Chen,[2] and Jong Heo[4]
[1]*The School of Materials Science and Chemical Engineering, Ningbo University, Ningbo, Zhejiang 315211, People's Republic of China*
[2]*Laboratory of Infrared Materials and Devices, Ningbo University, Ningbo, Zhejiang 315211, People's Republic of China*
[3]*State Key Laboratory of Silicate Materials for Architectures (Wuhan University of Technology), 122 Luoshi Road, Hongshan, Wuhan, Hubei 430070, People's Republic of China*
[4]*Center for Information Materials, Department of Materials Science and Engineering, Pohang University of Science and Technology, Pohang, Gyeongbuk 790-784, South Korea*

(Received 7 April 2012; accepted 21 May 2012; published online 8 June 2012)

We report the fabrication and characterization of $80GeS_2{\cdot}20Ga_2S_3{:}0.5Tm_2S_3$ chalcogenide glass-ceramics. A careful thermal process has led to the formation of ~50 nm Ga_2S_3 nanocrystals. By monitoring the $^3H_5 \rightarrow {}^3F_4$ Tm^{3+} transition, an almost fivefold increase of in the intensity and ~76 μs prolongation in the lifetime of mid-infrared fluorescence at 3.8 μm have been observed after crystallization. Element mapping evidenced that enhancement in the mid-infrared emission intensity was related to the formation of Ge-rich region in the glass-ceramics, consistent with spectroscopic results from glasses with different levels of GeS_2 content and β-GeS_2 precipitation. © *2012 American Institute of Physics*. [http://dx.doi.org/10.1063/1.4727900]

With their favorable properties such as wide transparency window (up to 22 μm), high refractive index, and low phonon energy, chalcogenide glasses doped with rare earth ions (REI) continue to attract widespread attention because of their potential applications in lasers, amplifiers, high-brightness sources for remote sensing, and spectroscopy.[1–4] In particular, the low phonon energy of chalcogenide glasses (~150–450 cm^{-1}) allows many mid-infrared (IR) transitions of REI normally quenched in silica (~1100 cm^{-1}) and fluoride (560 cm^{-1}) glasses to be active, which contributes to the unique optoelectronic potential in the mid-IR spectral range. Since the first report on mid-IR emission in REI-doped chalcogenide glasses was published,[5] intensive research has been conducted on the potential of solid-state mid-IR lasers, including spectroscopic studies on their bulk and fiber forms.[6–10] Bright mid-IR sources have been achieved as an alternative to globar sources in spectrometers and as bright sources for hardware-in-the-loop testing.[11,12] Recently, spectroscopic studies[7,8] and modeling[12] of REI doped chalcogenide glasses have demonstrated that laser action can be achieved in the 3–5 μm wavelength range. To date, however, lasing is still limited in near IR range,[3] and no extension to the mid-IR range is available. Efficient approaches are therefore required to enhance the mid-IR fluorescence of REI-doped chalcogenide glass.

Controlling the chemical environment of the REI through crystallization is an efficient way to enhance luminescence efficiency. The enhanced luminescence in REI-doped transparent glass-ceramics, combined with the favorable properties of crystal and glass matrix, has attracted worldwide interest, and researcher efforts have led to great progress.[13–15] Enhanced fluorescence can be obtained in low-loss oxide glass-ceramic waveguides, making them quite a promising component in integrated optoelectronic devices.[15] Moreover, similar behavior can be observed in REI-doped chalcogenide glass-ceramics. Luminescence increases more than 10 times in transparent glass-ceramics compared with base glass.[16–18] However, research on this effect on the mid-IR transitions of REI is scarce. The fundamental mechanism on the enhancement of mid-IR emission upon crystallization still remains largely unknown since precipitation of nanocrystals in the glass not only changes the composition of the residual glass matrix but also the local environment of REI.

In this Letter, we performed a spectroscopic study of Tm^{3+}-doped Ge-Ga-S chalcogenide glass-ceramics that revealed an enhanced mid-IR transition. Thulium ion was especially selected due to its fluorescence at 3.8 μm,[19] which coincides with an atmospheric transmission window for potential remote-sensing applications. Additionally, Ga-containing chalcogenide glass has been recognized as a superior host due to its large REI solubility and is regarded as relevant to mid-IR lasers.[8] Based on the spectroscopic and compositional mapping analyses using electron energy loss spectroscopy (EELS), mechanism responsible for the enhancement of mid-IR emission from Tm^{3+} doped chalcogenide glass-ceramics was proposed.

Bulk glass with a composition of $80GeS_2{\cdot}20Ga_2S_3{:}0.5Tm_2S_3$ (GGT-20) was prepared by melt-quenching method. The glass rod was annealed, cut into discs (Φ10 mm × 2 mm), and optically polished. The as-prepared glass discs was ceramized by heating at 2 °C/min to a designated temperature (T_{HT} = 458 °C)[20] and were held for various durations. Optical absorption and transmission spectra were recorded with a PerkinElmer-LAMBDA 950 UV/VIS/NIR

a)Author to whom correspondence should be addressed. Electronic mail: daishixun@nbu.edu.cn.

 © 2012 American Institute of Physics

This article is copyrighted as indicated in the article. Reuse of AIP content is subject to the terms at: http://scitation.aip.org/termsconditions. Downloaded to IP: 141.223.173.110 On: Wed, 22 Apr 2015 08:35:40

spectrophotometer in the visible and near-IR (Vis-NIR) range and by a Nicolet 380 FT-IR spectrometer, respectively. The mid-IR fluorescence spectra in the range of 2000–4100 nm were measured through a computer-controlled system consisting of a Zolix Omni-λ3015 monochromator with a SCITEC Model 420 lock-in amplifier and an InSb detector (DInSb 55-De) cooled with liquid nitrogen. A Ti:sapphire laser (Coherent Mira 900-D) at 800 nm was used as an excitation beam. All measurements were taken at room temperature. The crystalline phases precipitated in the heat-treated samples were identified using x-ray diffraction (XRD) and by comparing with the JCPDF cards of standard crystals. Room-temperature XRD was performed on powder samples with a conventional θ–θ Bragg–Brentano configuration (Cu $K_{\alpha 1,2} = 1.5406$ Å) on a Bruker D2 Phaser diffractometer fitted with a linear LynxEye^{TM} detector. Crystals in a glassy matrix were observed by TEM–STEM technique. A Cs-corrected HR-(S)TEM (JEM-2200FS) equipped with Ω-filter on the energy-filtered image was used for the EELS. The energy loss induced by the Ge: L_3, Ga: L_3, S: $L_{2,3}$, Tm: $N_{4,5}$ shell electron was detected in the mapping of elements in the glass.

Figure 1 presents the Vis-NIR absorption spectra of the obtained samples. Several absorption bands are assigned to the electron transitions from the ground states of Tm^{3+}:$^3H_6$ to the indexed excited ones. The location and spectral shape of the absorption bands are similar to those of Ga-La-S glasses.[19] As shown in Fig. 1, the cut-off edge of the short wavelength highly sensitive to the presence of crystals red-shifts gradually with annealing time, indicating the formation and growth of nanocrystals in the GGT-20 base glasses. Fortunately, the presence of crystals does not impair the transparency in the application window located at mid-IR spectral region from 2 to 10 μm as shown in the inset of Fig. 1, especially at 3.8 μm of the mid-IR transition of Tm^{3+} ions.

Figure 2 shows the XRD patterns of the GGT-20 as-prepared glass and glass-ceramics. Some sharp diffraction peaks assigned to the crystal phase Ga_2S_3 (JCPDF card No. 84-1441) arise from the broad vitreous profile. These diffraction peaks are coincident with those of the crystallized samples without RE ions.[20,21] Thus, it can be supposed that Tm^{3+} ions are not involved in the nucleation and crystal growth of Ga_2S_3 crystals. Further investigation and discussion are presented in the following sections. The inset of Fig. 2 presents the microstructure of the glass-ceramic sample as observed by STEM, which reveals that the ~50 nm crystals are formed uniformly in the glass matrix.

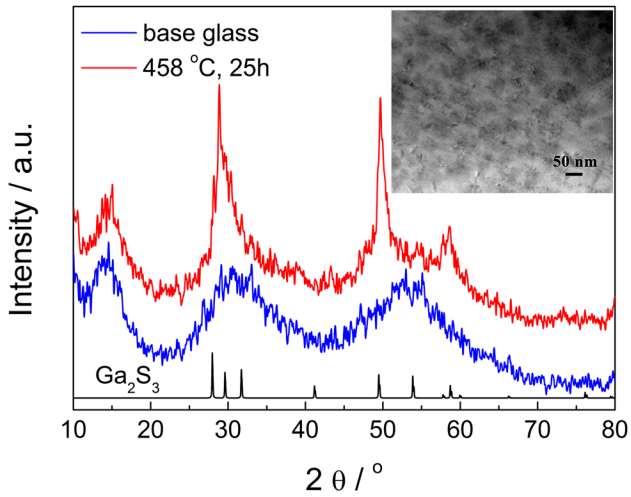

FIG. 2. XRD patterns of as-prepared GGT-20 glass and glass-ceramics after the heat treatment at 458 °C for 25 h. The inset shows the STEM image of the glass-ceramic sample.

The mid-IR emission spectra of Tm^{3+}-doped glass and glass-ceramics were measured with an excitation wavelength of 0.8 μm from a Ti:sapphire laser. Excitation at 0.8 μm populates the $^3H_4$ level, and subsequently, the $^3H_5$ and $^3F_4$ levels by means of radiative and nonradiative transitions. In particular, the transition of $^3H_5 \rightarrow {}^3F_4$ that gives fluorescence at 3.8 μm can be observed, as presented in Fig. 3. It cannot be realized in fluoride and oxide glasses because of a much stronger nonradiative multiphonon decay to the $^3H_5 \rightarrow {}^3F_4$ transition. Furthermore, the fluorescence intensity is remarkably enhanced in crystallized samples. Despite the higher scattering losses at excitation (as shown in Fig. 1), the emission intensity is highly dependent on the heat-treatment duration. The strongest fluorescence at 3.8 μm, which is nearly

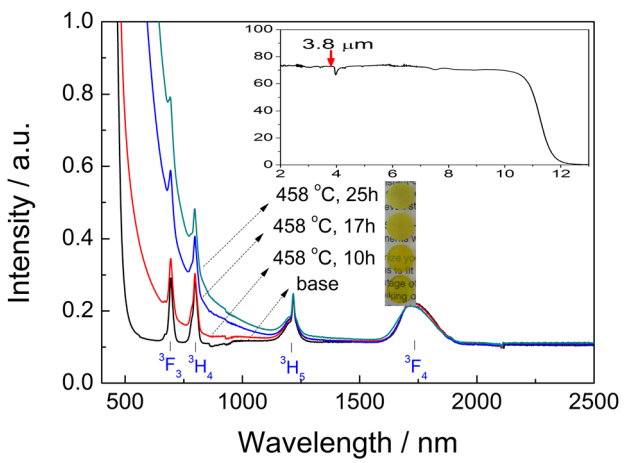

FIG. 1. Vis-NIR absorption spectra of GGT-20 glass crystallized at 458 °C for different durations: 0, 10, 17, and 25 h, respectively. The inset is the typical mid-IR transmission spectrum for base and crystallized glasses.

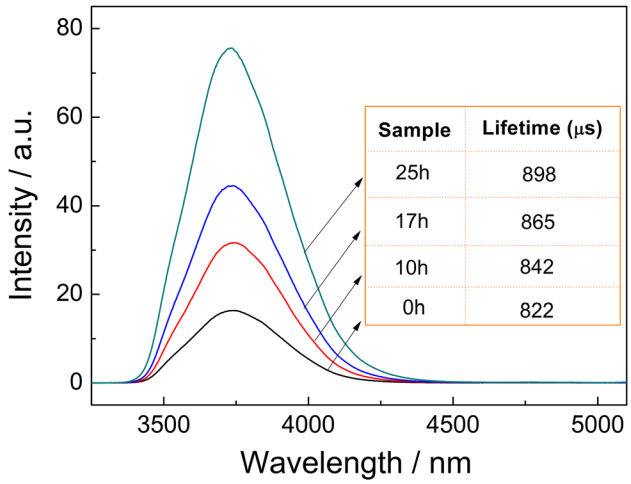

FIG. 3. Mid-IR emission spectra of the GGT-20 glass samples crystallized at 458 °C for different durations: 0, 10, 17, and 25 h, respectively. The inset lists the fluorescence lifetime of 3.8 μm for each sample.

This article is copyrighted as indicated in the article. Reuse of AIP content is subject to the terms at: http://scitation.aip.org/termsconditions. Downloaded to IP: 141.223.173.110 On: Wed, 22 Apr 2015 08:35:40

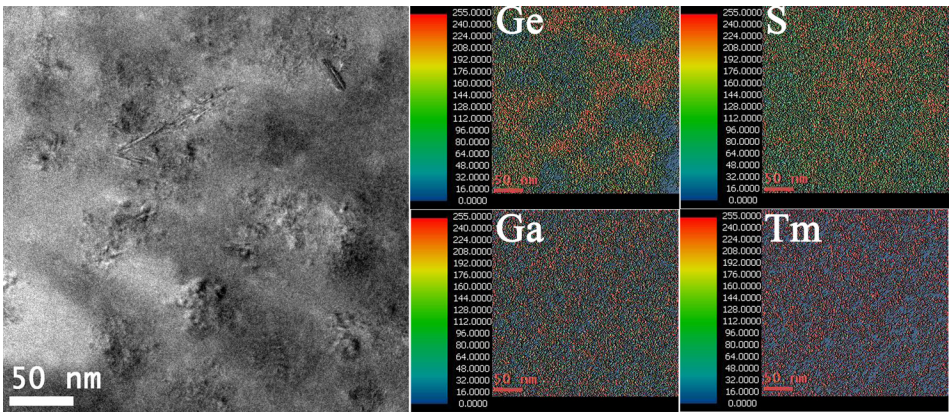

FIG. 4. HAADF image and Ge, S, Ga, and Tm EELS elemental maps of GGT-20 glass crystallized at 458 °C for 25 h obtained by the integration method.

five times higher than that of the host glass, was obtained in the crystallized sample after 25 h of heat treatment. In addition, the fluorescence lifetime was measured by pumping the samples at 0.8 μm. The $^3H_5$ level was measured by observing the decay around 3.8 μm. The inserted table in Fig. 3 lists the fluorescence lifetimes of GGT-20 glass and glass-ceramics, which were obtained by fitting the fluorescence decay curves with the exponential decay function. It shows that the fluorescence lifetimes are ranging from 822 to 898 μs and elongate with heat-treatment time. The longer fluorescence lifetime is believed to result in the higher gain. The enhanced fluorescence intensity and lifetime are reflected by the local structural change around Tm^{3+} ions after heat treatment, making it promising as a mid-IR laser medium for transitions originating from that level.

As demonstrated, there has been a remarkable evolution of mid-IR fluorescence in glass and glass-ceramics, which may be partly due to the contribution of the changed local environments of Tm^{3+}, such as the crystalline and low phonon energy nanostructure like that in the oxyfluoride glass-ceramics.[14,22] However, this study presents a different outcome. A suitable enhanced mechanism of mid-IR fluorescence should be considered in these REI-doped chalcogenide glass-ceramics. No fluorescence line-narrowing indicates that the Tm^{3+} ions do not reside at crystal sites. The lifetime of an excited state is governed by a combination of probabilities for all possible radiative and nonradiative transitions, as described in the following equation:[23]

$$\tau^{-1} = \tau_R^{-1} + W_{\mathrm{MP}} + W_{\mathrm{ET}}, \qquad (1)$$

where τ_{R} is the radiative lifetime and W_{MP} and W_{ET} are the probabilities of nonradiative relaxation due to multiphonon relaxation and energy transfer to the neighbor ions, respectively. In this study, the REI concentration (0.5 mol. % as Tm^{3+}) does not reach the doping limitation that can exceed 1 mol. % in GeS_2-Ga_2S_3 glasses. The contribution of crystallization to W_{ET} can be ignored. Therefore, W_{MP} is responsible for the longer fluorescence lifetime in crystallized samples. The fluorescence lifetime and intensity both increase with the decreasing photon energy of the local environment of Tm^{3+} ions during the crystallization.

To check the local fluctuation of elements (or phonon energy) originating from the crystallization, we employed EELS in HR-STEM for the elemental mapping of Ge, S, Ga, and Tm.[24,25] The simultaneously acquired high-angle annular dark-field (HAADF) image is shown in Fig. 4. The main characteristics of the crystallized sample are as expected, with Ge more concentrated in the crystal-free area (glass matrix) of the HAADF image and a large amount of S present everywhere. There are similar EELS maps of Ga and Tm in almost equal proportions all over the image. Tm elements do not aggregate with the precipitation of Ga_2S_3 crystallite, which is in accordance with the no fluorescence line-narrowing as shown in Fig. 3. However, the Ga is rather noisy. In particular, the correlation of increase in Ga concentration with the crystal zones in the HAADF image is somewhat tenuous. The poor quality of the Ga image compared with that of Ge is caused by the limitation of the conventional background power law model. The signal of Ga-L_3 edge centered at 1115 eV is difficult to extract from the broad background of the Ge-L_3 edge. Even so, it is sure that the Tm^{3+} ions do not participate in the crystallization of Ga_2S_3. The apparent variation in Ge content from place to place as mapped in Fig. 4 is a strong indication of genuine local composition changes. Therefore, it is reasonable to assume that the compositional variation in the residual glass matrix, i.e., the low phonon energy of Ge-rich areas, results in lifetime and emission-intensity changes.

The aggregation of Ge in the EELS map is one proof that the measured fluorescence arises mostly from Tm^{3+} ions dispersed at the Ge-rich sites in the glass matrix. Another central observation from the above analysis is that, as shown in Fig. 5, the fluorescence intensity in $90GeS_2{\cdot}10Ga_2S_3$:$0.5Tm_2S_3$ (GGT-10) base glass is much larger than that in the GGT-20 one. Specifically, the increment of enhanced fluorescence in these base glasses is in accordance with that in the crystallized GGT-20 glasses. Meanwhile, previous work has revealed that transparent glass-ceramics embedding β-GeS_2 crystallite would be precipitated in $90GeS_2{\cdot}10Ga_2S_3$ glass through careful crystallization process.[26] It is therefore not surprising to see that the fluorescence intensity decreases with the heat treatments, as displayed in the inset of Fig. 5. These results further suggest that the formation of Ge-rich areas is more favorable to mid-IR fluorescence than the presence of crystallites in the glass matrix, which might indicate the benefit of phase separation of Ge-rich regions during crystallization.

In summary, transparent glass-ceramics containing Ga_2S_3 nanocrystals were fabricated through the ceramization of $80GeS_2{\cdot}20Ga_2S_3$:$0.5Tm_2S_3$ chalcogenide glass. Enhanced mid-IR fluorescence of nearly five times and prolonged lifetime of $\sim$76 μs were observed at room temperature. The

This article is copyrighted as indicated in the article. Reuse of AIP content is subject to the terms at: http://scitation.aip.org/termsconditions. Downloaded to IP: 141.223.173.110 On: Wed, 22 Apr 2015 08:35:40

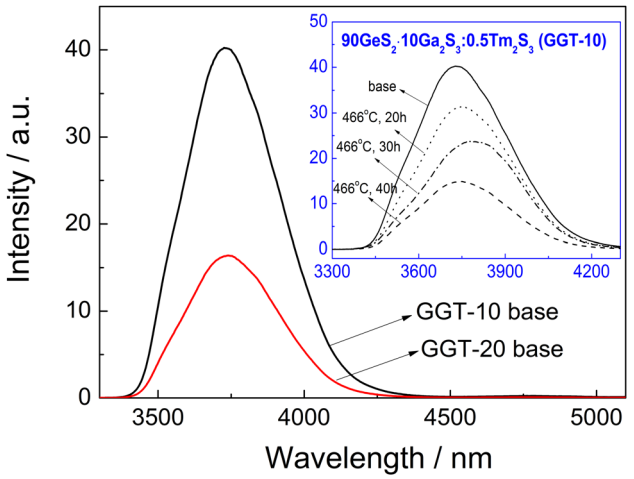

FIG. 5. Mid-IR emission spectra of the GGT-10 and GGT-20 base glasses. The inset is that of GGT-10 glass samples crystallized at 466 °C for different durations: 0, 20, 30, and 40 h, respectively.

beneficial effect of crystallization on Tm^{3+} fluorescence was demonstrated as a function of both heat-treatment time and GeS_2 content. The enhanced mechanism of mid-IR fluorescence in chalcogenide glass-ceramics was clearly evidenced as the phase separation of Ge-rich regions in the glass matrix during crystallization.

This work was partially supported by the International Science & Technology Cooperation Program of China (Grant No. 2011DFA12040), National Program on Key Basic Research Project (973 Program) (Grant No. 2012CB722703), the National Natural Science Foundation of China (Grant Nos. 61108057, 61177087, and 60978058), the Program for New Century Excellent Talents in University (Grant No. NCET-10-0976), the Zhejiang Provincial Natural Science Foundation of China (Grant Nos. R1101263, Q12E020013, and Y4110322), the Natural Science Foundation of Ningbo City (Grant No. 2011A610091), and the Program for Innovative Research Team of Ningbo City (Grant No. 2009B21007). It was also sponsored by K.C. Wong Magna Fund in Ningbo University. J. Heo was supported by Priority Research Centers Program (2011-0031405) and WCU (World Class University) program (R31-30005) through the National Research Foundation (NRF) funded by the Ministry of Education, Science and Technology of Korea, and the Collaborative Research Project under the NRF-Natural Science Foundation of China (NSFC) Cooperative Program (D00039).

[1]B. Fan, C. Point, J.-L. Adam, X. Zhang, X. Fan, and H. Ma, J. Appl. Phys. **110**(11), 113107–113108 (2011).
[2]A. Mori, Y. Ohishi, T. Kanamori, and S. Sudo, Appl. Phys. Lett. **70**(10), 1230–1232 (1997).
[3]T. Schweizer, D. W. Hewak, D. M. Payne, T. Jensen, and G. Huber, Electron. Lett **32**(7), 666–667 (1996).
[4]H. Tao, Z. Yang, and P. Lucas, Opt. Express **17**(20), 18165–18170 (2009).
[5]J. Heo, J. N. Jang, and Y. S. Kim, Proc. SPIE **1817**, 134–140 (1992).
[6]J. S. Sanghera, L. Brandon Shaw, and I. D. Aggarwal, IEEE J. Sel. Top. Quantum Electron. **15**(1), 114–119 (2009).
[7]V. Moizan, V. Nazabal, J. Troles, P. Houizot, J.-L. Adam, J.-L. Doualan, R. Moncorg, F. Smektala, G. Gadret, S. Pitois, and G. Canat, Opt. Mater. **31**(1), 39–46 (2008).
[8]A. B. Seddon, Z. Tang, D. Furniss, S. Sujecki, and T. M. Benson, Opt. Express **18**(25), 26704–26719 (2010).
[9]T. Schweizer, D. W. Hewak, B. N. Samson, and D. N. Payne, Opt. Lett. **21**(19), 1594–1596 (1996).
[10]L. Shaw, B. Harbison, B. Cole, J. Sanghera, and I. Aggarwal, Opt. Express **1**(4), 87–96 (1997).
[11]L. B. Shaw, B. J. Cole, J. S. Sanghera, I. D. Aggarwal, F. H. Kung, S. S. Bayya, R. Mossadegh, P. A. Thielen, J. R. Kircher, and J. R. L. Murrer, "Development of IR-emitting infrared fibers at the Naval Research Laboratory," Proc. SPIE **4366**, 90–95 (2001).
[12]R. S. Quimby, L. B. Shaw, J. S. Sanghera, and I. D. Aggarwal, IEEE Photon. Technol. Lett. **20**(2), 123–125 (2008).
[13]Q. Y. Zhang and X. Y. Huang, Prog. Mater Sci. **55**(5), 353–427 (2010).
[14]D. Chen, Y. Yu, P. Huang, F. Weng, H. Lin, and Y. Wang, Appl. Phys. Lett. **94**, 041909 (2009).
[15]S. N. B. Bhaktha, F. Beclin, M. Bouazaoui, B. Capoen, A. Chiasera, M. Ferrari, C. Kinowski, G. C. Righini, O. Robbe, and S. Turrell, Appl. Phys. Lett. **93**, 211904 (2008).
[16]R. Balda, S. García-Revilla, J. Fernández, V. Seznec, V. Nazabal, X. H. Zhang, J. L. Adam, M. Allix, and G. Matzen, Opt. Mater. **31**(5), 760–764 (2009).
[17]E. Guillevic, M. Allix, X. Zhang, J.-L. Adam, G. Matzen, and X. Fan, Mater. Res. Bull. **45**(4), 448–455 (2009).
[18]V. Seznec, H. L. Ma, X. H. Zhang, V. Nazabal, J.-L. Adam, X. S. Qiao, and X. P. Fan, Opt. Mater. **29**(4), 371–376 (2006).
[19]T. Schweizer, B. N. Samson, J. R. Hector, W. S. Brocklesby, D. W. Hewak, and D. N. Payne, J. Opt. Soc. Am. B **16**(2), 308–316 (1999).
[20]C. Lin, L. Calvez, M. Rozé, H. Tao, X. Zhang, and X. Zhao, Appl. Phys. A **97**, 713–720 (2009).
[21]C. Lin, L. Calvez, H. Tao, M. Allix, A. Moréac, X. Zhang, and X. Zhao, J. Solid. State Chem. **184**(3), 584–588 (2011).
[22]H. Lin, D. Chen, Y. Yu, A. Yang, and Y. Wang, Opt. Lett. **36**(6), 876–878 (2011).
[23]M. J. Weber, Phys. Rev. **157**(2), 262–272 (1967).
[24]R. F. Egerton, *Electron Energy-Loss Spectroscopy in the Electron Microscope* (Springer, 2011).
[25]C. Liu and J. Heo, "Electron Energy Loss Spectroscopy Analysis on the Preferential Incorporation of Er3+ ions into Fluoride Nanocrystals in Oxyfluoride Glass-Ceramics," J. Am. Ceram. Soc. (in press).
[26]C. Lin, L. Calvez, L. Ying, F. Chen, B. a. Song, X. Shen, S. Dai, and X. Zhang, Appl. Phys. A **104**(2), 615–620 (2011).

This article is copyrighted as indicated in the article. Reuse of AIP content is subject to the terms at: http://scitation.aip.org/termsconditions. Downloaded to IP: 141.223.173.110 On: Wed, 22 Apr 2015 08:35:40